

# Fractional Josephson vortices at $\text{YBa}_2\text{Cu}_3\text{O}_{7-x}$ grain boundaries

R. G. Mints and Ilya Papiashvili

*School of Physics and Astronomy,*

*Raymond and Beverly Sackler Faculty of Exact Sciences, Tel Aviv University, Tel Aviv 69978, Israel*

(November 19, 2018)

We report numerical simulations of magnetic flux patterns in asymmetric  $45^\circ$  [001]-tilt grain boundaries in  $\text{YBa}_2\text{Cu}_3\text{O}_{7-x}$  superconducting films. The grain boundaries are treated as Josephson junctions with the critical current density  $j_c(x)$  alternating along the junctions. We demonstrate the existence of Josephson vortices with fractional flux quanta for both periodic and random  $j_c(x)$ . A method is proposed to extract fractional vortices from experimental flux patterns.

Numerous recent studies of electromagnetic properties of grain boundaries in high- $T_c$  superconducting films are driven by necessity to probe the fundamental symmetry of the order parameter and the flux quantization [1–3]. Although interpretation of the results is nontrivial, most of the data can be understood in terms of the conventional model of a strongly coupled Josephson junction [4]. The asymmetric  $45^\circ$  [001]-tilt grain boundary in  $\text{YBa}_2\text{Cu}_3\text{O}_{7-x}$  films is a notable exception of this rule. We show in this letter that these boundaries should have unusual electromagnetic properties unprecedented for the physics of standard Josephson junctions.

Experimentally the asymmetric  $45^\circ$  [001]-tilt grain boundaries in  $\text{YBa}_2\text{Cu}_3\text{O}_{7-x}$  films exhibit an anomalous dependence of the critical current  $I_c$  on the applied magnetic field  $H_a$  [5,6]. Contrary to the usual Fraunhofer-type dependence with a major central peak at  $H_a = 0$  and minor symmetric side-peaks, these boundaries demonstrate a pattern without the central major peak. Instead, two symmetric major side-peaks appear at certain fields  $H_a = \pm H_p \neq 0$  [5–7]. Other remarkable feature is the spontaneous disordered magnetic flux generated at the asymmetric  $45^\circ$  [001]-tilt grain boundaries in  $\text{YBa}_2\text{Cu}_3\text{O}_{7-x}$  films [8]. It is worth noting that the spontaneous flux is observed only in samples exhibiting the anomalous dependence  $I_c(H_a)$ .

Clearly, the major side-peaks reveal a *specific* heterogeneity of the Josephson properties. Indeed, a fine scale faceting of grain boundaries in YBCO thin films has been recorded by the transmission electron microscopy [3,9–11]. The facets have a typical length-scale  $l$  of the order of 10–100 nm and a wide variety of orientations. This grain boundary structure combined with a predominant  $d_{x^2-y^2}$  wave symmetry of the order parameter [2,12–14] form a basis for understanding both the anomalous dependence  $I_c(H_a)$  and the spontaneous flux [7,8,15,16].

In the case of a  $d_{x^2-y^2}$  wave superconductor the phase difference of the order parameter across the grain boundary consists of two terms. The first term  $\varphi(x)$  is caused by a magnetic flux inside the junction and the second term  $\alpha(x)$  is caused by a misalignment of the anisotropic

banks of the junction. The Josephson current density  $j(x)$  depends on the total phase difference  $\varphi(x) + \alpha(x)$ . Assuming  $j(x) \propto \sin[\varphi(x) + \alpha(x)]$  one can develop a model of the electromagnetic properties of the grain boundaries in YBCO films [6]. Values of the phase  $\alpha(x)$  depend on the relative orientation of the neighboring facets. In the case of an asymmetric faceted  $45^\circ$  grain boundary we have an interchange of  $\alpha = 0$  and  $\pi$  and  $j(x) = j_c(x) \sin \varphi(x)$ , where the alternating critical current density  $j_c(x) \propto \cos \alpha(x)$ .

In this letter we report numerical simulations of flux patterns in the asymmetric  $45^\circ$  [001]-tilt grain boundaries in  $\text{YBa}_2\text{Cu}_3\text{O}_{7-x}$  superconducting films. The boundaries are treated as Josephson junctions with an alternating critical current density  $j_c(x)$ . We find two types of fractional Josephson vortices for each stationary state with a spontaneous flux in the grain boundaries, which exists for both periodic and random sequences of facets. One type of vortices contains the magnetic flux  $\phi_1 < \phi_0/2$ ; the other type carries  $\phi_2 > \phi_0/2$  with a complementarity condition  $\phi_1 + \phi_2 = \phi_0$ , where  $\phi_0$  is the flux quantum. We suggest a method to extract the fractional vortices from the data on flux patterns.

The alternating dependence  $j_c(x)$  is imposed by a particular sequence of facets along the boundary and therefore  $j_c(x)$  has the same typical length-scale  $l$  as the facets. It is convenient for the further analysis to write  $j_c(x)$  as

$$j_c = \langle j_c \rangle [1 + g(x)], \quad (1)$$

where  $\langle j_c \rangle$  is the average value of the critical current density over distances  $L \gg l$ :

$$\langle j_c \rangle = \frac{1}{L} \int_0^L j_c(x) dx. \quad (2)$$

The dimensionless function  $g(x)$  in Eq. (1) characterizes the Josephson properties of the grain boundary. This function alternates with a typical length-scale  $l$  and has a zero average:  $\langle g(x) \rangle = 0$ . The maximum amplitude of alternations of  $|g(x)|$  may vary from  $|g(x)|_{\max} \gtrsim 1$  to  $|g(x)|_{\max} \gg 1$  depending on details of the structure of the

faceted grain boundary. We assume that  $\lambda \ll l \ll \Lambda_J$ , where  $\lambda$  is the London penetration depth and

$$\Lambda_J^2 = \frac{c\phi_0}{16\pi^2\lambda\langle j_c \rangle}. \quad (3)$$

is an effective Josephson penetration depth. With this notation, the phase difference  $\varphi(x)$  satisfies

$$\Lambda_J^2 \varphi'' - [1 + g(x)] \sin \varphi = 0. \quad (4)$$

A model grain boundary with a periodic critical current density  $j_c(x)$  has been considered analytically by means of a two-scale perturbation theory which requires  $l \ll \Lambda_J$  [15]. In this approximation, the phase  $\varphi(x)$  is a sum of a smooth part  $\psi(x)$  with a length scale  $\Lambda_J$  and a rapidly oscillating part  $\xi(x)$  with a length scale  $l$  and a small amplitude  $|\xi(x)| \ll 1$ :

$$\varphi(x) = \psi(x) + \xi(x). \quad (5)$$

We have for the phases  $\psi(x)$  and  $\xi(x)$ :

$$\Lambda_J^2 \psi'' - \sin \psi + \gamma \sin \psi \cos \psi = 0, \quad (6)$$

$$\xi(x) = \xi_g(x) \sin \psi, \quad (7)$$

where the function  $\xi_g(x)$  is given by

$$\Lambda_J^2 \xi_g'' = g(x), \quad (8)$$

and the dimensionless parameter  $\gamma > 0$  is defined as

$$\gamma = -\langle g(x)\xi_g(x) \rangle = \Lambda_J^2 \langle \xi_g'^2 \rangle. \quad (9)$$

It is worth mentioning that both  $\xi_g(x)$  and  $\gamma$  depend only on the spatial distribution of  $j_c$  and therefore characterize the *individual* Josephson properties of a particular grain boundary. We stress that this approximation is valid if  $l \ll \Lambda_J$  and  $|\xi(x)| \ll |\psi(x)|$  (the latter condition results in  $|g(x)| \ll 4\pi^2\Lambda_J^2/l^2$ ).

In the framework of the two-scale perturbation theory, a single Josephson vortex is described by the solution of Eq. (6) under the boundary conditions  $\psi'(\pm\infty) = 0$ . The latter can be written as  $\sin \psi_{\pm} (1 - \gamma \cos \psi_{\pm}) = 0$ , where  $\psi_{\pm} = \psi(\pm\infty)$ . It is convenient for the further analysis to assume that  $\psi_- < \psi_+$ .

In the case of  $\gamma < 1$ , there is only one single vortex solution, for which the phase  $\psi(x)$  increases monotonically from  $\psi_- = 0$  to  $\psi_+ = 2\pi$ . This solution describes the Josephson vortex with one flux quantum  $\phi_0$ . In the case of  $\gamma > 1$ , the spatial distribution of the smooth phase  $\psi$  describes two fractional vortices. For the *first* fractional vortex the phase  $\psi(x)$  increases from  $\psi_- = -\psi_\gamma$  to  $\psi_+ = \psi_\gamma$ , where

$$\psi_\gamma = \arccos(1/\gamma). \quad (10)$$

The difference  $\psi_+ - \psi_- = 2\psi_\gamma$  and thus this vortex carries the flux  $\phi_1 = \psi_\gamma \phi_0 / \pi < \phi_0/2$ . For the *second* fractional

vortex  $\psi_- = \psi_\gamma$ ,  $\psi_+ = 2\pi - \psi_\gamma$ , the phase difference being  $2\pi - 2\psi_\gamma$ , and thus this vortex contains the flux  $\phi_2 = (1 - \psi_\gamma/\pi)\phi_0 > \phi_0/2$ . These two fractional vortices are *complementary*:  $\phi_1 + \phi_2 = \phi_0$ .

In our numerical study we solve Eq. (4) exactly. We treat the stationary states as well as the relaxation to the stationary states using a time-dependent model [16]

$$\ddot{\varphi} + \alpha \dot{\varphi} - \varphi'' + [1 + g(x)] \sin \varphi = 0, \quad (11)$$

where  $\alpha$  is a decay constant which we take from the interval  $0.1 < \alpha < 1$ . The term  $\alpha \dot{\varphi}$  in Eq. (11) describes dissipation driving the system into one of the stable stationary states described by the solutions of Eq. (4).

We begin our numerical simulations with verification of the results obtained by means of the two-scale approximation for the grain boundary with periodic  $j_c(x)$ . To study the fractional vortices we start the simulations from a certain initial phase  $\varphi_i(x)$  under the condition  $\varphi_i(\mathcal{L}) - \varphi_i(0) = 2\pi n$ , where the boundary length  $\mathcal{L} \gg \Lambda_J$ . In this case the numerical procedure converges well to a final stationary state.

In Fig. 1 we show a stable stationary solution for a pair of fractional vortices. We compute  $\varphi(x)$  using the model  $g(x) = g_0 \sin(2\pi x/l)$  with  $g_0 = 100$  and  $l = 0.1\Lambda_J$ . The value of  $\gamma$  calculated by means of Eq. (9) is given by

$$\gamma = \frac{g_0^2 l^2}{8\pi^2 \Lambda_J^2}. \quad (12)$$

This yields  $\gamma \approx 1.27$  and  $\psi_\gamma \approx 0.66$ ; thus  $\phi_1 \approx 0.21\phi_0$ ,  $\phi_2 \approx 0.79\phi_0$ . As is seen in Fig. 1, the simulation gives the same value of  $\psi_\gamma$ . The magnified insets in Fig. 1 demonstrate that  $\varphi(x)$  indeed consists of a smooth part superimposed with a small fast oscillating term. Therefore, the numerical simulations for single fractional vortices confirm the qualitative and quantitative results of the approximate analytic approach described above.

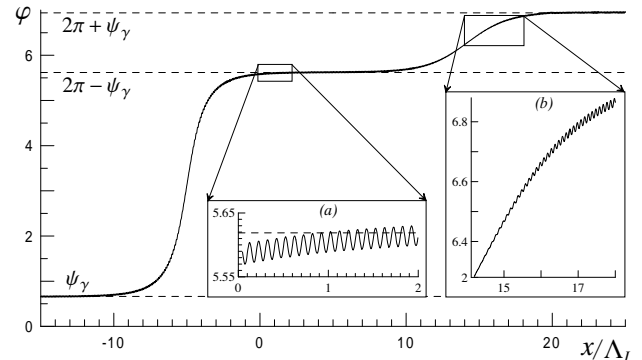


FIG. 1. The phase distribution  $\varphi(x)$  computed using  $g(x) = g_0 \sin(2\pi x/l)$  and  $\gamma \approx 1.27$ . Two fractional vortices with  $\phi_1 \approx 0.21\phi_0$  and  $\phi_2 \approx 0.79\phi_0$  are clearly seen, the fine structure of  $\varphi(x)$  is demonstrated in the magnified insets.

Consider now a dilute chain of fractional vortices. Let a vortex with the flux  $\phi_1$  be situated somewhere in the chain. The phase  $\psi$  of this vortex changes from  $2\pi n - \psi_\gamma$  to  $2\pi n + \psi_\gamma$  with an integer  $n$ . Therefore, one expects the phase of an adjacent vortex to start with the value  $2\pi n + \psi_\gamma$  and to end up with  $2\pi(n+1) - \psi_\gamma$ , the total phase accumulation of these two vortices being  $2\pi$ . In other words, the chain consists of a sequence of pairs of vortices with fluxes  $\phi_1$  and  $\phi_2$ . This qualitative picture is confirmed by numerically solving Eq. (4). Figure 2(a) shows the result of such a calculation for which we took  $g(x) = 150 \sin(20\pi x/\Lambda_J)$ , that corresponds to  $\gamma \approx 2.85$ ,  $\psi_\gamma \approx 1.21$ , and the fluxes  $\phi_1 \approx 0.39\phi_0$ ,  $\phi_2 \approx 0.61\phi_0$ . The final stationary state of our numerical procedure simulating the relaxation process, depends on the choice of the initial phase  $\varphi_i(x)$ . By taking a proper non-monotonic dependence  $\varphi_i(x)$ , we may end up with a stationary solution shown in Fig. 2(b). A remarkable feature of this solution is the existence of *fractional vortex-antivortex pairs* clearly seen in the simulation of Fig. 2(b), the pair with the fluxes  $\pm\phi_1$  is followed by the pair with  $\mp\phi_2$ .

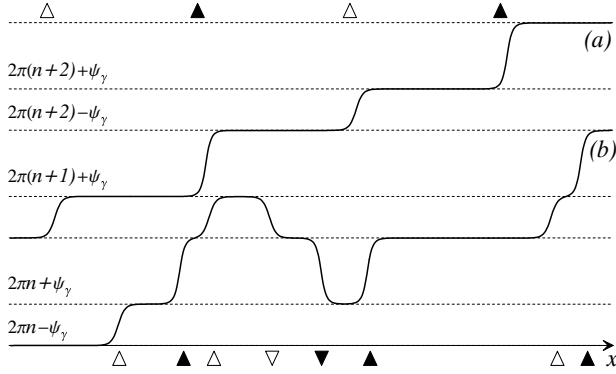


FIG. 2. Two chains of fractional vortices in a grain boundary with a periodically alternating critical current density: (a) an “ideal” chain, (b) a chain with vortex-antivortex “defects”. Empty triangles mark the positions of the fractional vortices with the fluxes  $\phi_1 < \phi_0/2$ , full triangles correspond to  $\phi_2 > \phi_0/2$ . The up-down orientation of triangles indicate the field direction of vortices. For this particular calculation we use  $g(x) = g_0 \sin(2\pi x/l)$ ,  $g_0 = 150$ ,  $l = 0.1 \Lambda_J$ , which result in  $\gamma \approx 2.85$ ,  $\psi_\gamma \approx 1.21$ , and  $\phi_1 \approx 0.39\phi_0$ ,  $\phi_2 \approx 0.61\phi_0$ .

Next, we study flux patterns for a more realistic case of a grain boundary with  $2N$  facets and a non-periodic alternating critical current density  $j_c(x)$ . We treat this case numerically and use a stepwise  $g(x)$  defined as:  $g(x) = g_0$  if  $a_i < x < b_i$ , and  $g(x) = -g_0$  if  $b_i < x < a_{i+1}$  ( $i = 1, \dots, N$ ). It is convenient to introduce the random distances  $\tilde{a}_i$  and  $\tilde{b}_i$  with  $\langle \tilde{a}_i \rangle = \langle \tilde{b}_i \rangle = 0$  and a standard deviation  $\sigma_l$  such that  $b_i - a_i = 0.5(l + \tilde{a}_i)$  and  $a_{i+1} - b_i = 0.5(l + \tilde{b}_i)$ . The simulations start with an initial phase  $\varphi_i(x)$  matching the condition  $\varphi_i(\mathcal{L}) - \varphi_i(0) = 2\pi n$ . Then the numerical procedure of solving Eq. (11) converges well to a stationary state which depends on

both  $\varphi_i(x)$  and  $\alpha$  due to the flux pinning induced by the non-uniformity of the critical current density.

A special role in the description of Josephson boundaries with random alternating  $j_c(x)$  belongs to the stationary state  $\varphi_s(x)$  which corresponds to the zero total spontaneous flux and to the absolute minimum of the Josephson energy  $\mathcal{E}\{\varphi(x)\}$  (defined in a standard way [17]). Our simulations show that  $\varphi_s(x)$  is *unique* for a given boundary, *stable*, and *independent* either of initial guesses  $\varphi_i(x)$  or of the damping constant  $\alpha$ . Therefore, the phase  $\varphi_s(x)$  can serve as a *signature* of each individual boundary. It is convenient to represent  $\varphi_s(x)$  as  $\varphi_s(x) = \psi_\gamma + \xi_s(x)$  with  $\psi_\gamma = \text{const}$  and the variable part  $\xi_s(x)$  having zero average,  $\langle \xi_s(x) \rangle = 0$ , and a typical amplitude  $|\xi_s(x)| < \pi/2$ .

An example of a computed  $\varphi_s(x)$  is shown in Fig. 3(a). For this simulation we took  $\varphi_i(x) = \text{const} + \xi_i(x)$  with an arbitrary small  $\xi_i(x)$ . As stated above, the resulting phase  $\varphi_s(x)$  is independent of  $\varphi_i(x)$ . It is worth mentioning that the spontaneous self-generated flux  $\phi_s(x) = \phi_0 \xi_s(x)/2\pi$  has a wide range of length-scales imposed by the random  $j_c(x)$ . Note also that randomness of  $j_c(x)$  results in a considerably higher amplitude of the flux variation  $\phi_s(x)$  as compared to a periodic  $j_c(x)$ ; this is seen from comparison of Fig. 3(a) with the insets in Fig. 2.

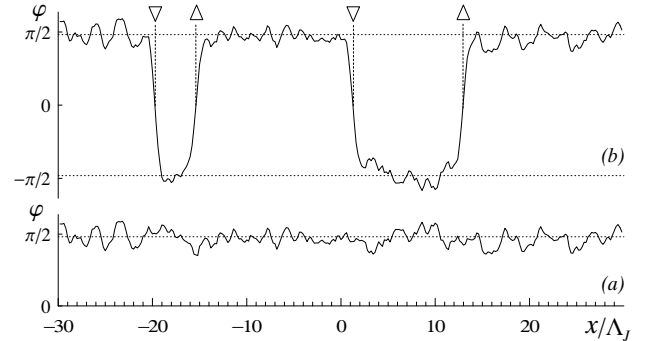


FIG. 3. Two stationary solutions  $\varphi(x)$  developed in a zero magnetic field for a stepwise randomly alternating  $g(x)$  for two initial conditions: (a) preventing, (b) stimulating creation of vortices ( $g_0 = 200$ ,  $l = 0.1 \Lambda_J$ ,  $\sigma_l \approx 0.06l$ ,  $\psi_\gamma \approx 1.515$ ,  $\phi_1 \approx 0.48\phi_0$ ,  $\phi_2 \approx 0.52\phi_0$ ).

It follows from Eq. (4) that the stationary solution  $\varphi_s(x)$  generates two series of solutions having the same Josephson energy as  $\varphi_s(x)$ :  $\varphi_n^+(x) = 2\pi n + \varphi_s(x)$  and  $\varphi_n^-(x) = 2\pi n - \varphi_s(x)$ , where  $n$  is an integer. The average values  $\langle \varphi_n^+(x) \rangle = 2\pi n + \psi_\gamma$  and  $\langle \varphi_n^-(x) \rangle = 2\pi n - \psi_\gamma$  interchange being separated by  $\langle \varphi_n^+(x) \rangle - \langle \varphi_n^-(x) \rangle = 2\psi_\gamma$  or by  $\langle \varphi_{n+1}^-(x) \rangle - \langle \varphi_n^+(x) \rangle = 2\pi - 2\psi_\gamma$ , as is shown in Fig. 2 for a periodic  $j_c(x)$ . The gaps between the average values of the stationary phases  $\varphi_n^+(x)$  and  $\varphi_n^-(x)$  allow for fractional vortices with the fluxes  $\phi_1 = \phi_0 \psi_\gamma/\pi$  and  $\phi_2 = \phi_0 - \phi_1$  as solutions of Eq. (4) varying with a typical length-scale of  $\Lambda_J$ . An example of a computed  $\varphi(x)$  with two clearly pronounced fractional vortex-antivortex

pairs and small varying part  $\xi(x)$  is shown in Fig. 3(b).

Consider now a typical flux (phase) pattern for a chain of vortices for a randomly alternating  $j_c(x)$ . Assume that the chain starts with a domain with  $\varphi(x) = \varphi_s(x)$ , *i.e.*, the phase varies slightly ( $|\xi_s(x)| < \pi/2$ ) around its average value  $\psi_\gamma$ . Therefore,  $\psi_\gamma$  is the value of  $\langle \varphi(x) \rangle$  at the “tail” of the neighboring vortex or antivortex. If the neighbor carries the flux  $\phi_2$ , the average phase should increase from  $\psi_\gamma$  to  $2\pi - \psi_\gamma$  in the neighbor’s domain. Alternatively the neighbor may carry the flux  $-\phi_1$  generating a decrease of  $\langle \varphi(x) \rangle$  from  $\psi_\gamma$  to  $-\psi_\gamma$ . In general, this flux pattern is similar to the one arising for a periodic  $j_c(x)$ . However, the relatively large amplitudes of the spontaneous flux and the absence of periodicity within the chain may mask the fractional vortices.

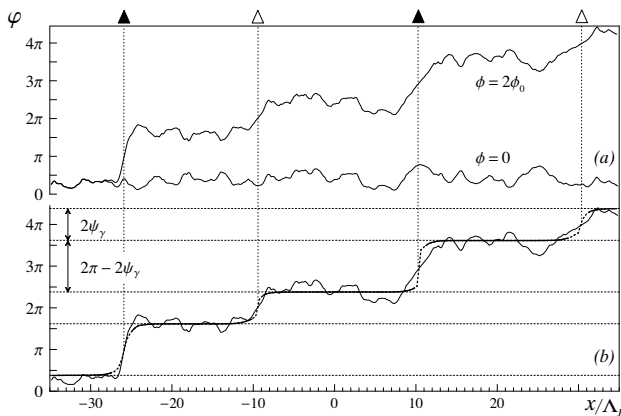


FIG. 4. (a) The “signature”  $\varphi_s(x)$  and the phase  $\varphi(x)$  with the total flux  $\phi = 2\phi_0$  at the boundary calculated for  $g_0 = 90$ ,  $l = 0.1\Lambda_J$ ,  $\sigma_l \approx 0.015l$ , which gives  $\psi_\gamma \approx 1.21$ , and  $\phi_1 \approx 0.39\phi_0$ ,  $\phi_2 \approx 0.61\phi_0$ . (b) The thin line depicts  $\varphi(x)$ , the thick line depicts the phase  $\varphi_v(x)$  generated by the fractional vortices and extracted from the phase  $\varphi(x)$ .

At the top panel of Fig. 3 we show  $\varphi(x)$  obtained numerically for  $g_0 = 90$ ,  $l = 0.1\Lambda_J$ , and  $\sigma_l = 0.015l$ , the calculated value of  $\psi_\gamma$  is 1.21. The bottom curve is the “signature”  $\varphi_s(x)$  corresponding to the zero total flux,  $\phi = 0$ . The upper curve is calculated with the same set of input parameters for  $\phi = 2\phi_0$ . Even a brief examination of the curves shows a striking correlation between the two: there are domains (e.g.,  $-10 < x/\Lambda_J < 10$ ) in which the “noise” patterns are nearly identical, whereas in others (e.g.,  $10 < x/\Lambda_J < 30$ ) the patterns repeat each other being flipped. This suggests that one can extract the smooth part of the upper curve  $\varphi(x)$  by properly subtracting the “signature”  $\varphi_s(x)$ .

The subtraction is done as follows. First, we draw the straight lines  $2\pi n \pm \psi_\gamma$  at the graph of  $\varphi(x)$ , see Fig. 4(b). We see that “random” variations of  $\varphi(x)$  are nested on

one of these lines everywhere, except a few relatively sharp jumps from one line to the next; in particular, the “signature”  $\varphi_s(x)$  is nested at  $\psi_\gamma$ :  $\varphi_s(x) = \psi_\gamma + \xi_s(x)$ . The jumps (or vortices) should be centered at  $\varphi(x) = \pi n$  [where according to Eq. (4)  $\varphi''(x) = 0$ ]. Then we take a domain situated between lines  $\pi n$  and  $\pi(n+1)$  and form  $\varphi_v(x) = \varphi(x) \mp \xi_s(x)$ , choosing the minuses if the random parts of  $\varphi(x)$  and  $\varphi_s(x)$  are identical, and the plus otherwise. The curve  $\varphi_v(x)$  shown by a thick curve at Fig. 4(b) is remarkably *smooth*; clearly it represents the fractional vortices described above within the model with periodic  $j_c(x)$ .

In conclusion, we have shown by numerical simulations that two types of fractional vortices with fluxes  $\phi_1 < \phi_0/2$  and  $\phi_2 = \phi_0 - \phi_1 > \pi/2$  exist at  $45^\circ$  [001]-tilt grain boundaries in  $\text{YBa}_2\text{Cu}_3\text{O}_{7-x}$  films exhibiting spontaneous flux in zero field cooled samples. Faceted grain boundaries are treated as Josephson junctions with alternating critical current density. We show how to extract fractional vortices from the data on spontaneous flux distribution.

One of us (RGM) is grateful to J.R. Clem, V.G. Kogan, and J. Mannhart for useful and stimulating discussions. This research is supported in part by grant No. 96-00048 from the United States – Israel Binational Science Foundation (BSF), Jerusalem, Israel.

- 
- [1] P. Chaudhari and S.Y. Lin, Phys. Rev. Lett. **72**, 1084 (1994).
  - [2] C.C. Tsuei *et al.*, Phys. Rev. Lett. **73**, 593 (1994).
  - [3] J.H. Miller *et al.*, Phys. Rev. Lett. **74**, 2347 (1995).
  - [4] R. Gross *et al.*, Phys. Rev. Lett. **64**, 228 (1990).
  - [5] C.A. Copetti *et al.*, Physica C **253**, 63 (1995).
  - [6] H. Hilgenkamp, J. Mannhart, and B. Mayer, Phys. Rev. B **53**, 14586 (1996).
  - [7] R.G. Mints and V.G. Kogan, Phys. Rev. B **55**, R8682 (1997).
  - [8] J. Mannhart *et al.*, Phys. Rev. Lett. **77**, 2782 (1996).
  - [9] C.L. Jia *et al.*, Physica C **196**, 211 (1992).
  - [10] S.J. Rosner, K. Char, and G. Zaharchuk, Appl. Phys. Lett. **60**, 1010 (1992).
  - [11] C. Træholt *et al.*, Physica C **230**, 425 (1994).
  - [12] D.A. Wollman *et al.*, Phys. Rev. Lett. **71**, 2134 (1993).
  - [13] D.A. Brawner and H.R. Ott, Phys. Rev. B **50**, 6530 (1994).
  - [14] D.J. Van Harlingen, Rev. Mod. Phys. **67**, 515 (1995).
  - [15] R.G. Mints, Phys. Rev. B **55**, R8682 (1997).
  - [16] R.G. Mints and Ilya Papiashvili, Phys. Rev. B **62**, 15214 (2000).
  - [17] A. Barone and G. Paterno, *Physics and Applications of the Josephson Effect* (Wiley, New York, 1982).